Inorganic Chemistry

pubs.acs.org/IC

Article

Catalytic Formation of Coordination-Based Self-Assemblies by Halide Impurities

Eduard. O. Bobylev, Bas de Bruin, and Joost N. H. Reek*

Cite This: *Inorg. Chem.* 2021, 60, 12498−12505

Read Online

ACCESS | Metrics & More | Article Recommendations | Supporting Information

ABSTRACT: The dynamics of metal organic polyhedra (MOP) play a crucial role for their application in catalysis and host−guest chemistry and as functional materials. In this contribution, we study the influence of possible contaminations of different metal precursors on the kinetic properties of MOP. Exemplary five different MOP are studied with metal precursors of varying quality. The metal precursors are either obtained from commercial sources or prepared by various literature procedures. Studies into the self-assembly process using ^{1}H NMR and MS analyses were performed on Pt_2L_4, Pd_2L_4, Pd_6L_{12}, $Pd_{12}L_{24}$, and Ni_4L_6 assemblies. Commonly found impurities are shown to play a prominent role guiding selective formation of MOP, as they allow for an escape from otherwise kinetically trapped intermediates. The energy requirement for selective sphere formation is significantly lowered in many examples providing evidence for a catalytic role of halide impurities/additives in the self-assembly process. Furthermore, even though most analytical features such as ^{1}H NMR and MS analyses show identical results for assemblies with different types of metal precursors, the dynamics of formed assemblies differs significantly if slightly less pure starting materials are used. Tiny amounts of halide contaminations make the MOP more dynamic, which can play an important role for substrate diffusion especially if bulky substrates are used. We believe that this study on the influence of impurities (which were shown to be present in some commercial sources) on the kinetic properties of MOP together with procedures of obtaining high purity metal precursors provides important information for future material preparation and provides a better understanding of already known examples.

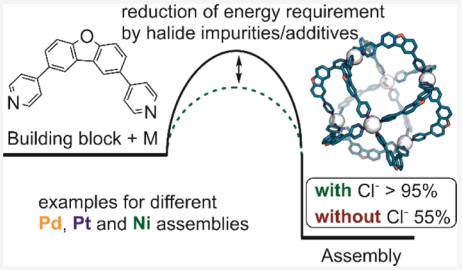

INTRODUCTION

Metal organic polyhedra (MOP) represent a class of nanosized three dimensional materials with an inner cavity.[1−9] Depending on the applied linker and the metal center, which are used to prepare the assemblies, a variety of different shapes can be obtained. The formation pathway proceeds through reversible bond formation between the metal and ligand, leading to the thermodynamically most favored structures due to geometric constraints. Most MOP are formed by applying a multidentate ligand and metal ions with a preferred coordination geometry. Prominent examples of MOP include spherical objects with the general composition M_nL_{2n}, $M_nL_{1.5n}$, M_nL_n, and $M_nL_{2/3n}$ (Figure 1).[10−18] The applied ligands have commonly multiple coordination sites, which allows for the formation of 3D-shaped objects. Depending on the applied metal center, different types of ligand donors have been demonstrated to be suitable candidates for the formation of MOP. As such, the list of possible ligands includes nitrogen donors such as pyridine, imidazole, and triazole;[1,3] oxygen donors such as aryl acids or phenols;[18−21] carbon donors such as N-heterocyclic carbenes,[22−24] and many more. The metal precursors are chosen, such that only certain structures are allowed due to geometric constraints. Typically, square planar or octahedral coordination modes are preferred (such as for Fe^{2+}, Co^{2+}, Ni^{2+}, Pd^{2+}, Pt^{2+}, and Zn^{2+}).[3,6,13,25−27] The so-formed spheres find a variety of applications in which they can act as a host for catalytic transformations or as a separation vehicle.[6,15,28−30] Through specific functionalization of the applied building blocks, unique properties are obtained by preorganization of functional groups, leading to materials with unique spectroscopic, catalytic, and physiological attributes.[30−34]

A key property for these materials of importance for applications is their kinetic stability. Through the implementation of multiple metal−ligand bonds, MOP display generally relatively rigid structures in comparison to the analogue monomers.[35,36,39] At certain points, however, the bond between the metal and ligand has to be broken to allow for the escape from kinetically trapped assemblies during the formation of specific spheres.[25,36] Likewise, the dynamic behavior of MOP is important in the context of catalytic transformations, as it can lead to better diffusion of the substrate in and the product out.

When we prepared MOP from commercially available metal precursors from various suppliers, the outcome of the synthesis

Received: June 6, 2021
Published: July 30, 2021

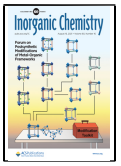

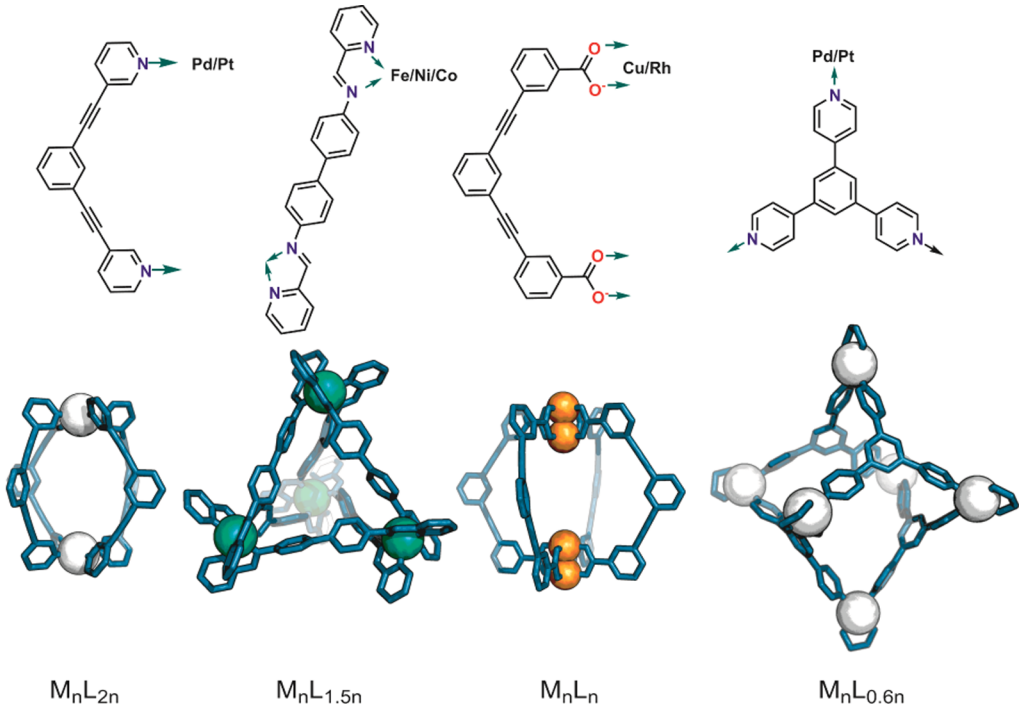

Figure 1. Representative examples for different stoichiometries in self-assembled metal organic polyhedral structures. Ligand frameworks are shown in green and metal centers as different colored spheres.

and the properties of MOP differed. Intrigued by irreproducible results of sphere formation, we identified the impurity responsible for it and studied the effect of possible impurities of different metal precursors on the self-assembly process and the kinetic properties of the resulting spheres.

In this contribution, we report the impact of precursor purity on formation and kinetics of self-assembled structures based on strong (Pt_2L_4 and Ni_4L_6) and weaker (Pd_2L_4, Pd_6L_{12}, and $Pd_{12}L_{24}$) metal–ligand bonds. With this contribution, we show that self-assembling processes are catalyzed by the presence of halide impurities, lowering the overall energy requirements for selective sphere formation. This not only provides insights into already known self-assembly processes but also paves the way for the formation of new materials under mild conditions.

RESULTS AND DISCUSSION

Synthesis of Metal Precursors. Diverse applied Fujita-type palladium- and platinum-based assemblies and Nitschke-type M_4L_6 assemblies were chosen for our investigations. Metal precursors of the general formula $[M(BF_4)_2(MeCN)_4]$ for M = Pd, Pt, and Ni were thus required. $[Pd(BF_4)_2(MeCN)_4]$ was purchased from different suppliers (Sigma-Aldrich and Strem, herein called $\mathbf{Pd}^{SA}$ and $\mathbf{Pd}^{S}$). Moreover, all precursors were prepared via different experimental procedures. Coordination of halides to metals typically kinetically labilized coordination-based materials. To study this, metal precursors were prepared via two slightly different routes. One set of metal precursors were obtained by addition of HBF_4 to the corresponding acetylacetonate (acac) precursors. Because this synthesis does not contain any halides, significant contamination with halides can be excluded ($\mathbf{Pd}^{Free}$, $\mathbf{Pt}^{Free}$, and $\mathbf{Ni}^{Free}$, Figure 2). The second synthetic route to metal precursors proceeds via the halide abstraction of MCl_2 complexes using $AgBF_4$. As the second route contains halides as precursors, it is more prone for halide impurities ($\mathbf{Pd}^{Halide}$, $\mathbf{Pt}^{Halide}$, and $\mathbf{Ni}^{Halide}$, Figure 2).

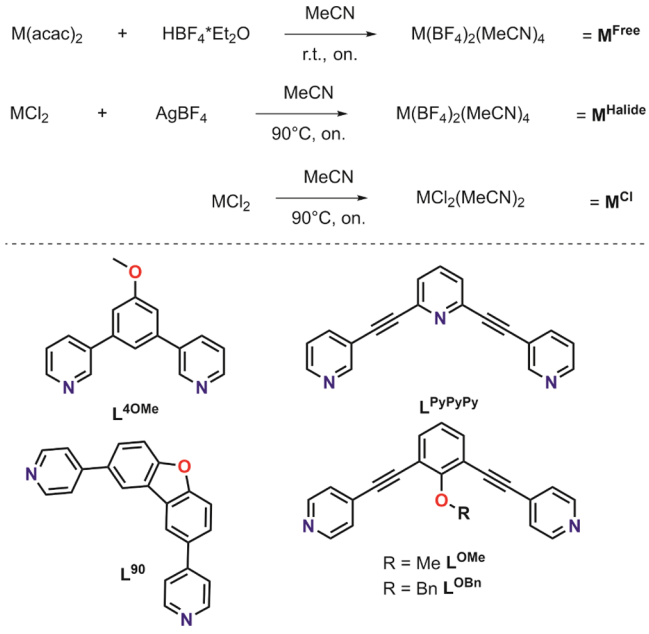

Figure 2. Synthesis route for the required metal precursors (for M=Ni, Pd, and Pt) and structure of the herein studied ligands.

For control purposes, $[MCl_2(MeCN)_2]$ complexes were prepared according to literature-known procedures ($\mathbf{Pd}^{Cl}$, $\mathbf{Pt}^{Cl}$, and $\mathbf{Ni}^{Cl}$, Figures 2, see S1).

All ligands required for our study were prepared according to standard organic synthesis protocols (Figure S2). The set contains two building blocks with pyridine donors with a bend angle of 0° ($\mathbf{L}^{PyPyPy}$ and $\mathbf{L}^{4OMe}$), which can be used for the assembly of the M_2L_4 type of spheres with palladium and platinum. One novel building block with a bend angle of 90°, which can be used for the assembly of Pd_6L_{12} assemblies ($\mathbf{L}^{90}$).

https://doi.org/10.1021/acs.inorgchem.1c01714
Inorg. Chem. 2021, 60, 12498−12505

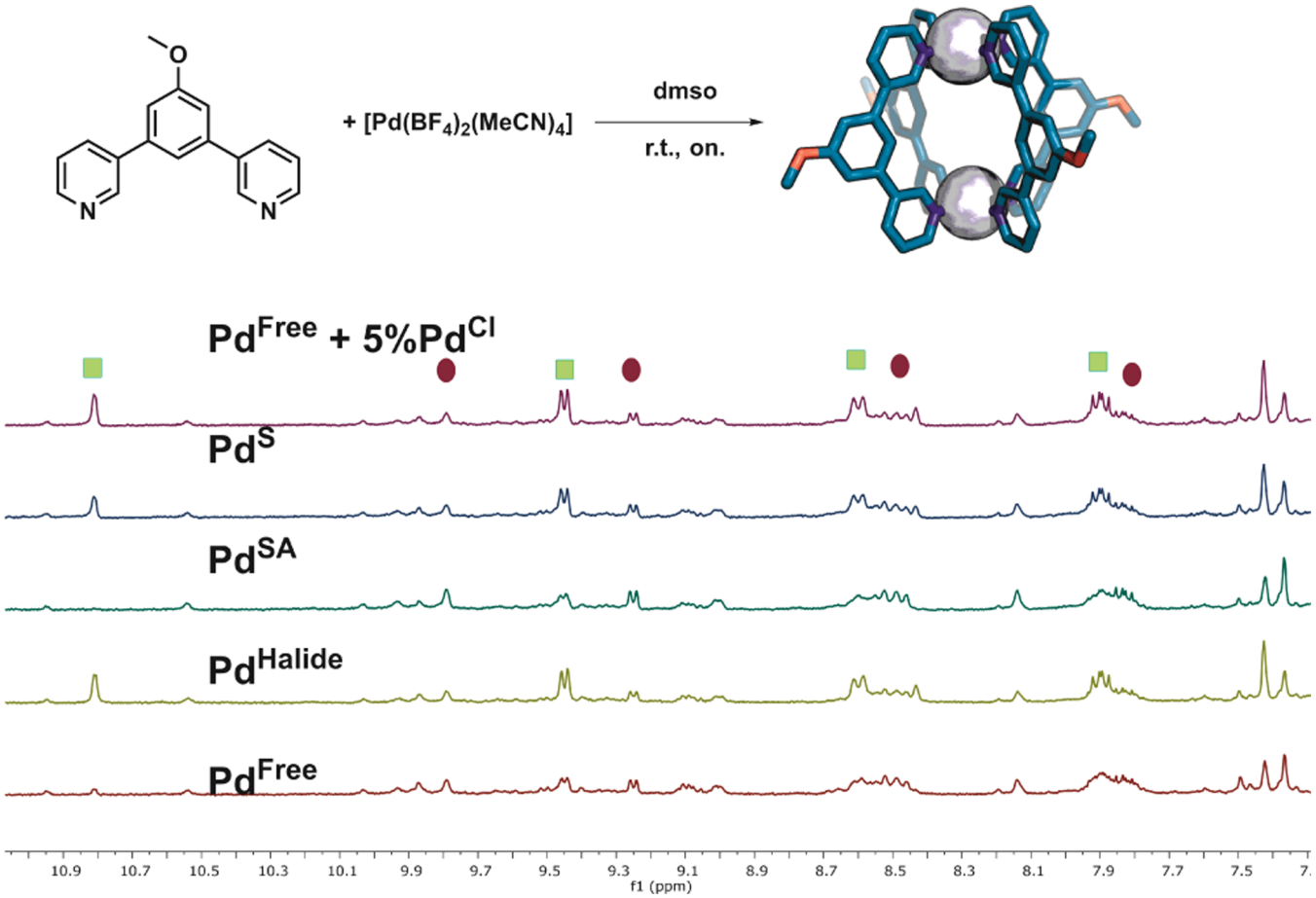

Figure 3. General scheme for the synthesis of $Pd_2L^{4OMe}{}_4$ assemblies. ^{1}H-NMR of the formed structure (green= M_2L_4 assembly and purple= M_4L_8).

Two building blocks of a third type with a bend angle of 120° for the formation of $M_{12}L_{24}$ assemblies (L^{OMe} and L^{OBn}) are shown in Figure 2. Benzidine and 2-pyridinecarboxyaldehyde were commercially available and can be used for the assembly of the M_4L_6 type of assemblies with different metal precursors.

Influence on the Self-Assembly Process of Pd_nL_{2n} Assemblies. First, a relatively simple $Pd_2L^{4OMe}{}_4$ assembly was studied. Sphere formation was performed by mixing 1 equiv L^{4OMe} with 0.55 equiv of different palladium precursors (Pd^S, Pd^{SA}, Pd^{Free}, and Pd^{Halide}). After stirring the solutions at room temperature for 24 h, the mixtures were analyzed by ^{1}H NMR and ESI-MS. ^{1}H NMR showed characteristic signals associated with the desired M_2L_4 assembly only for Pd^S and Pd^{Halide} (Figure 3). Besides the set of signals, which we attribute to the desired M_2L_4 assembly, a second set of signals was pronounced in ^{1}H NMR. By MS analysis, two different types of assemblies were identified. The major species in MS analysis is attributed to the desired M_2L_4 assembly. The second set of ^{1}H NMR signals corresponds to an M_4L_8 assembly, which was according to MS present in small quantities (Figures S13 and S14). Importantly, the signals associated with the desired M_2L_4 assembly are only visible when Pd^S and Pd^{Halide} are used as precursors, and samples prepared using Pd^{SA} or Pd^{Free} yield no M_2L_4 assembly at room temperature. By addition of 5% Pd^{Cl} to Pd^{Free} and consecutive sphere formation at room temperature, similar quantities of the desired M_2L_4 assembly were obtained as with Pd^{Halide} and Pd^S, indicating that chloride only needs to be present in catalytic amounts (Figure 3). Heating the solutions of Pd^{Free} or Pd^{SA} to 100 °C overnight also yields M_2L_4 assemblies, and it leads to comparable results as the reaction at room temperature in the presence of chloride (S15). The M_2L_4 assembly is considered therefore as the thermodynamic product of the self-assembly process. Halogen poor metal precursors such as Pd^{Free} and Pd^{SA} most likely get stuck in kinetic traps when the reaction is carried out at room temperature. As shown, addition of halides (Pd^{Cl}) or using precursors that contain halide impurities (herein Pd^{Halide} and Pd^S) allows for an escape from otherwise kinetically trapped states under mild conditions (for a clean synthetic procedure for the preparation of this type of assemblies, we would like to refer to ref 37). Because from this set of experiments, it is not clear if the chloride impurity has an influence on only the kinetic properties or if templating also may play a role (chloride binding in the small interior of the sphere is possible), a second assembly with a bigger interior volume was studied. For this purpose, complexation of a novel building block L^{90} was performed with all different metal precursors (Pd^{Free}, Pd^S, Pd^{SA}, Pd^{Halide}, and Pd^{SA} + 5% Pd^{Cl}). After complexation, the halide-rich palladium precursors (Pd^{Halide}, Pd^S, and Pd^{SA} + 5% Pd^{Cl}) displayed one sharp set of signals in ^{1}H NMR (Figure 4). The structure was assigned to $Pd_6L^{90}{}_{12}$, as supported by MS analysis (Figures S18 and S19). The halogen-poor palladium precursors Pd^{SA} and Pd^{Free} yield a mixture of two different assemblies being $Pd_5L^{90}{}_{10}$ and $Pd_6L^{90}{}_{12}$, as supported by ^{1}H NMR and MS analyses in a 1 to 1 ratio (Figures 4 and S20−21). Increasing the reaction temperature caused decomposition of the materials in solution before one single assembly was formed. As such, pure $Pd_6L_{12}{}^{90}$

https://doi.org/10.1021/acs.inorgchem.1c01714
Inorg. Chem. 2021, 60, 12498−12505

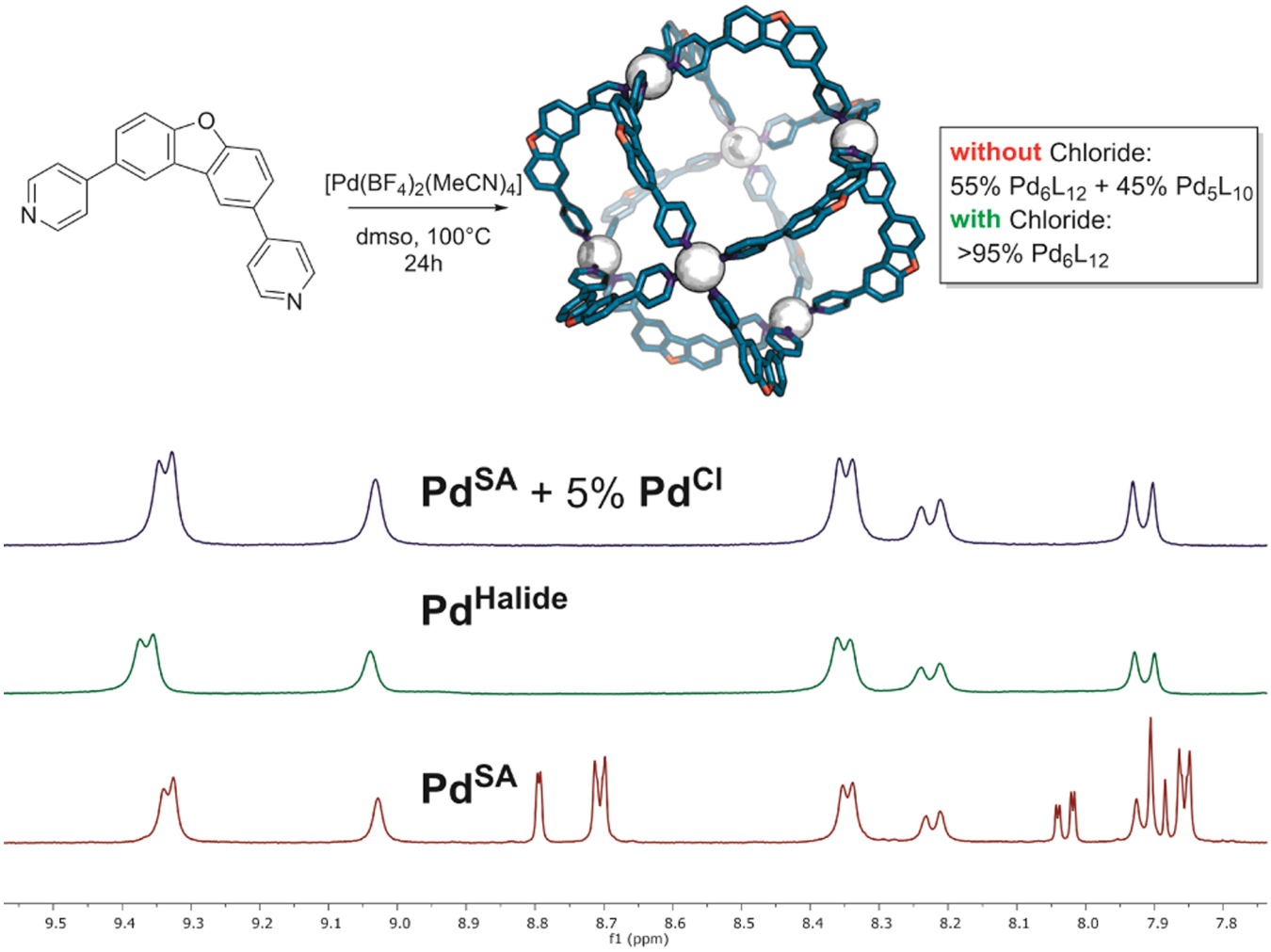

Figure 4. General scheme for the synthesis of $Pd_6L^{90}{}_{12}$ assemblies. ^{1}H-NMR of the formed assemblies using different metal precursors.

assemblies can only be obtained when a catalytic amount of chloride is present. Sphere formation studies on L^{4OMe} and L^{90} show that chloride impurities play a crucial role in guiding the self-assembly process of palladium-based systems. An escape from kinetically trapped intermediates was observed when less pure palladium precursors were used or halides were added on purpose. Because $Pd_2L^{4OMe}{}_4$ can be formed at enhanced temperature but not at low temperature, halides were found to reduce the energetic requirements for sphere formation, acting as a catalyst. For the more challenging novel $Pd_6L^{90}{}_{12}$ assembly, chloride additives/impurities have shown to be a determining factor in terms of selective formation (otherwise, a mixture of assemblies is obtained). Herein, it is important to mention that, qualitatively, a higher chloride level was determined using ESI-MS (S5) for Pd^S than for Pd^{SA} and for Pd^{Free}. However, as we demonstrated before, in principle, the presence of other strongly coordinating impurities such as alkyl acids can facilitate the formation of self-assemblies and cannot be fully excluded as contamination agents in the precursor Pd^S.[25]

To study the effect of the chloride impurities on the kinetic stability of the sphere after formation, two sets of $Pd_{12}L_{24}$ assemblies were studied. Sphere formation was performed by mixing either L^{OMe} or L^{OBn} with different palladium precursors (Pd^S, Pd^{SA}, and Pd^{Halide}) at 50 °C for 24 h. ^{1}H NMR of spheres prepared from Pd^{SA}, Pd^S, Pd^{Halide}, or Pd^{Free} + Pd^{Cl} showed quantitative formation of the desired assemblies by a downfield shift of the pyridine protons upon coordination to palladium (e.g., Figure S24). In contrast to that, the $[Pd_{12}L^{OMe}{}_{24}]$ assembly using Pd^{Free} was formed with a yield of 75% (Figure S24). Quantitative MS analysis showed the successful sphere formation by displaying a number of peaks corresponding to different charged states of $Pd_{12}L_{24}{}^{x+}$ for x = 6−13 (Figure S23). Furthermore, quantitative MS confirmed only 72 ± 7% of the $[Pd_{12}L^{OMe}{}_{24}]$ assembly for Pd^{Free} (ST1). As no other signals were detected in ^{1}H NMR or MS analysis, we suspect that the rest of the building block is involved in formation of oligomers. To obtain information, where consequences arise from using different types of metal precursors for the self-assembly, we analyzed the effect of the impurities on the kinetic stability of the such-formed assemblies by ligand exchange studies between two assemblies with different ligands. Two spheres were mixed in a 1 to 1 ratio and stirred at room temperature. The exchange of the ligands was monitored by quantitative MS analysis (Figures 5; see S4 for details). Assemblies prepared with Pd^{SA} showed 50% ligand exchange after 122 h. In contrast, assemblies prepared with less pure palladium precursors (such as Pd^S and Pd^{Halide}) already showed 71 and 76% ligand exchange. To confirm that halide impurities can cause such a drastic change in dynamics of the prepared self-assemblies, 5% Pd^{Cl} was added to Pd^{SA} and the so-formed spheres were mixed and studied over time. After

https://doi.org/10.1021/acs.inorgchem.1c01714
Inorg. Chem. 2021, 60, 12498−12505

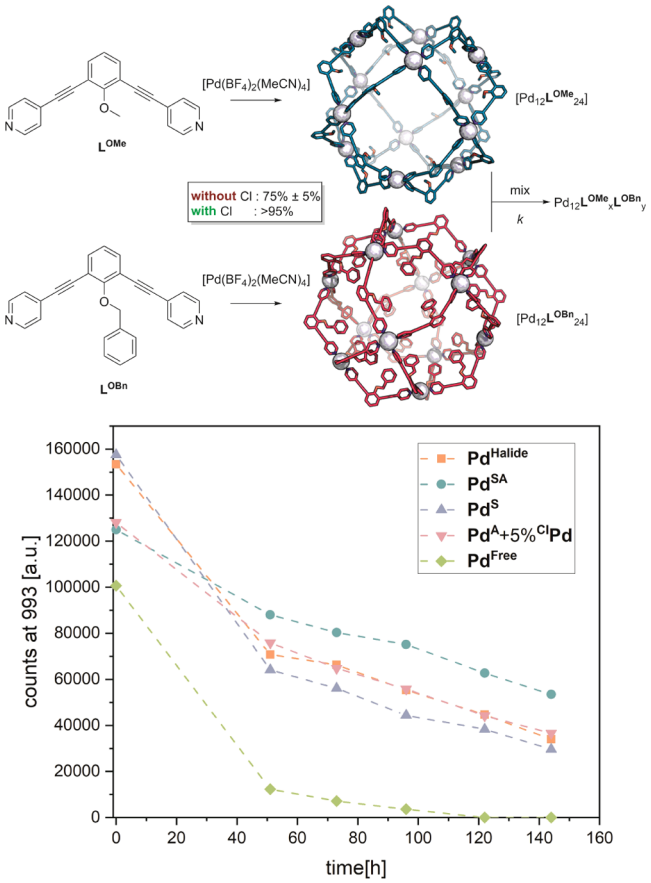

Figure 5. Representation of two $Pd_{12}L_{24}$ assemblies with different endo functionalities. The required palladium precursor was used from different suppliers for each set of exchange studies. Upon mixing of the two assemblies, the ligand exchange rate between the assemblies was monitored using quantitative MS. The graphic below shows the decay of the pure $\mathbf{L}^{\mathbf{OMe}}$ assembly.

122 h, 66% ligand exchange was observed to be in the same range of exchange as the other two metal precursors. Interestingly, after 2 d, an assemblies prepared from $\mathbf{Pd}^{\mathbf{Free}}$ showed almost full exchange of the building blocks (Figures 5, S33). As we previously demonstrated, the exchange of ligands between different assemblies with oligomers can proceed without any barrier.[25] As 25 ± 7% of the assemblies prepared from $\mathbf{Pd}^{\mathbf{Free}}$ is supposedly trapped in an oligomeric state, rapid ligand exchange was observed. Halide impurities were therefore shown to have a significant influence on the dynamics of assemblies after sphere formation and can potentially play an important role in avoiding diffusion limitations and enabling guest uptake for processes that require reversible Pd−nitrogen coordination when large guests are of interest (e.g., fullerenes).[38,39] In order to form robust self-assemblies, a fine balance of the added amount of halides is important, as it should be sufficient for the selective formation, but not exceeding it, as it enhances the dynamics of the formed spheres.

Influence on the Other Self-Assembly Process. Studies into other types of assemblies were performed. As MOP with strong metal−ligand bonds are generally formed at a higher temperature, a bigger influence by small halide impurities was expected. We studied Pt_2L_4 and Ni_4L_6 assemblies, which display the kinetically more robust analogues of palladium and iron assemblies.[33,40−43] Complexation of $\mathbf{L}^{\mathbf{PyPyPy}}$ with halide-free $\mathbf{Pt}^{\mathbf{Free}}$ yields the desired $Pt_2\mathbf{L}^{\mathbf{PyPyPy}}{}_4$ assembly at 150 °C (Figure 6). When the same procedure is performed at 90 °C with $\mathbf{Pt}^{\mathbf{Free}}$, only 70% of the desired structure is formed, as evidenced by multiple peaks in the aromatic region of the ^{1}H NMR spectrum (Figure 6). In contrast, the same sphere formation protocol at 90 °C with $\mathbf{Pt}^{\mathbf{Halide}}$ yields selectively the desired $Pt_2\mathbf{L}^{\mathbf{PyPyPy}}{}_4$ assembly (Figure 6). The same results are obtained also by addition of 2% $\mathbf{Pt}^{\mathbf{Cl}}$ to $\mathbf{Pt}^{\mathbf{Free}}$ and consecutive sphere formation (Figure 6). As such, we conclude that small amounts of halide impurities can drive the selectivity of small-sized platinum-based assemblies. Because many reported protocols rely on a platinum precursor prepared by chloride abstraction in situ similar to $\mathbf{Pt}^{\mathbf{Halide}}$, we anticipate the selective formation of the desired structures at temperatures lower than 150 °C due to trace impurities in the applied platinum precursor, which are able to catalyze selective sphere formation.

For nickel-based Ni_4L_6 assemblies, we observed a similar trend. Due to the paramagnetic nature of the resulting spheres, quantitative MS analysis was performed on the structures formed with either $\mathbf{Ni}^{\mathbf{Free}}$, $\mathbf{Ni}^{\mathbf{Halide}}$, or $\mathbf{Ni}^{\mathbf{Free}}$ + 5%$\mathbf{Ni}^{\mathbf{Cl}}$ (Figure 7). The correlation factor between the amounts of counts in MS and the concentration of the nickel assembly was obtained by calibration from a pure Ni_4L_6 assembly obtained by slow vapor diffusion of di-isopropyl ether into a solution of the assembly in acetonitrile (details Figure S4). The sphere formation protocol performed for 24 h at room temperature, instead of the typically used 90 °C to study the effect of the nickel precursor, showed significant differences based on the type of metal precursor. Samples using $\mathbf{Ni}^{\mathbf{Free}}$ provided the desired assembly in 7%. Both other nickel precursors $\mathbf{Ni}^{\mathbf{Halide}}$ and $\mathbf{Ni}^{\mathbf{Free}}$ + 10% $\mathbf{Ni}^{\mathbf{Cl}}$ showed better resolved MS spectra with 17 and 31% of the desired assembly in solution. In this scenario, two possible roles can be attributed to the presence of halides. $\mathbf{Ni}^{\mathbf{Cl}}$ can facilitate the dynamics of both, the nickel-ligand bonds and of the imine de/formation. Thus, all three metal−ligand systems provide support for a catalytic behavior of chloride additives/impurities for different types of coordination-based self-assembly processes (Figure 8). We envision that intermediate structures of the general formula ML_x are more dynamic in the presence of coordinating halides. These additives can open an alternative formation pathway proceeding through $ML_{x-1}Cl$ intermediates, which was shown to provide spheres at lower temperatures than typically required (Figure 8). This pathway is in accordance with the recently reported pathway using 2-chloropyridine.[44,45] However, catalytic amounts of halides have shown to be sufficient (in contrast, 2-chloropyridine is used superstoichiometrically).

CONCLUSIONS

In summary, we have identified a prominent contribution of halide impurities in applied metal precursors (or added on purpose) in the formation of MOP. Also, the dynamic properties of MOP, that is, exchange of ligand building blocks after formation, can be influenced by the presence of chloride anions, and they may stem from impurities in the metal precursor used. It was shown that self-assembled structures based on both strong (Pt) and weaker (Pd) metal−ligand bonds only form under mild conditions when a sufficient amount of the halide is present. The halide impurities allowed for an escape from otherwise kinetically trapped intermediates. Many of the herein presented assemblies can be formed at an elevated temperature without the presence of halides.

https://doi.org/10.1021/acs.inorgchem.1c01714
Inorg. Chem. 2021, 60, 12498−12505

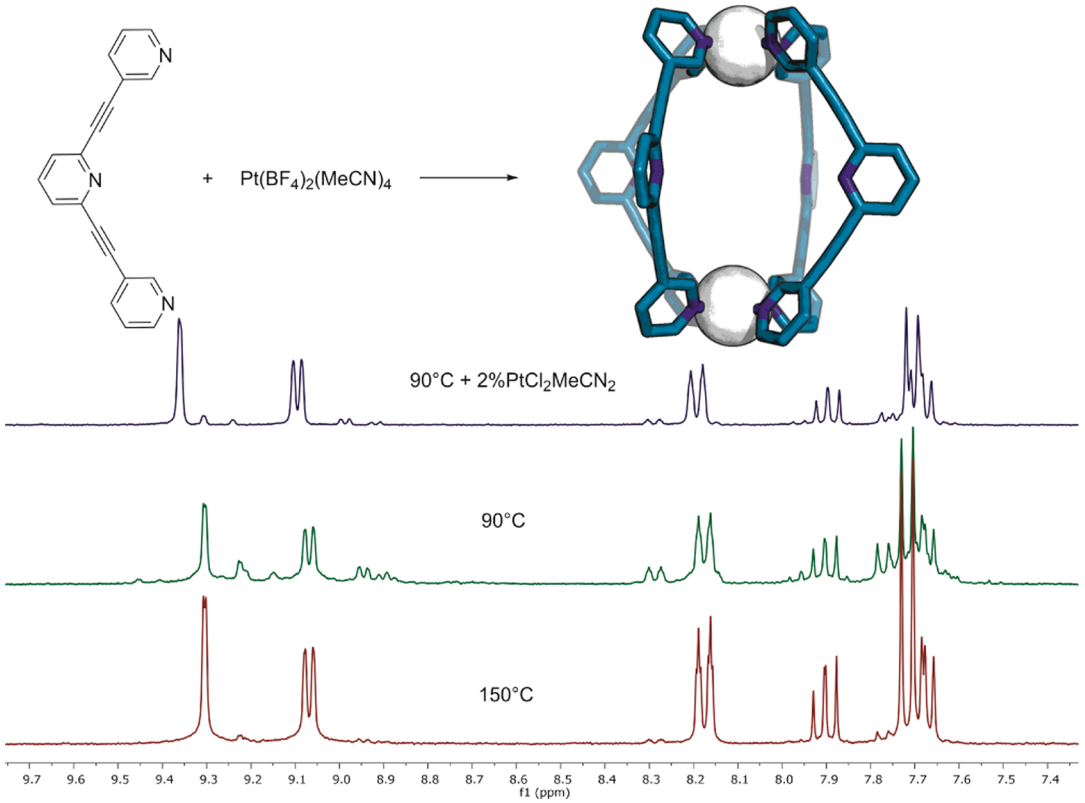

Figure 6. Sphere formation of Pt_2L_4 assemblies at different temperatures (150 and 90 °C). ^{1}H-NMR of the self-assemblies, at 150 °C (bottom), at 90 °C with halide addition (2% Pt^{Cl}) (top), and at 90 °C without halides (middle).

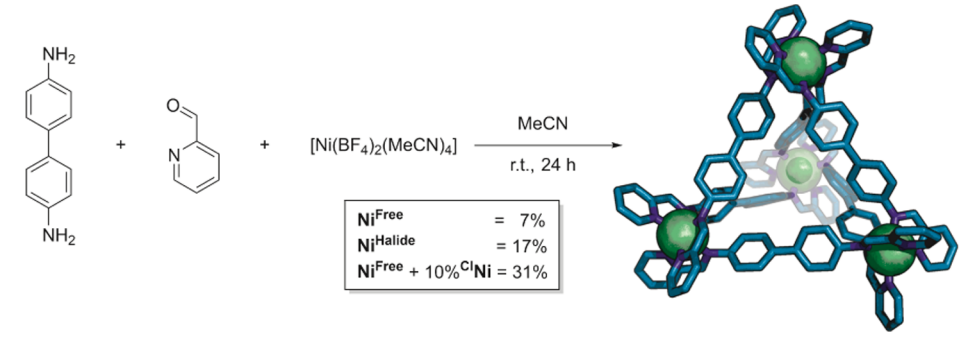

Figure 7. Sphere formation of Ni_4L_6 assemblies with different nickel precursors. Yields of the assemblies were obtained by quantitative MS analysis.

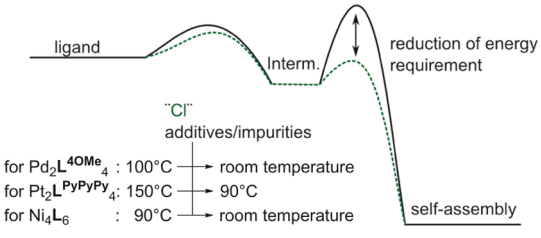

Figure 8. Qualitative representation of the proposed reduction of the energy barrier required to obtain self-assemblies by the presence of the catalytic amount of halides (green).

However, small amounts of halide additives/impurities lower the barrier for sphere formation significantly and can thus act as a catalyst for the formation of coordination-based self-assemblies. In one case, a selective formation of the Pd_6L_{12} assembly was not possible at all without the presence of chloride. The required amount for selective sphere formation can be found in some commercially available metal precursors, leading to possibly different results of the self-assembly depending on the obtained precursor batch. We want to emphasize that a clean method is presented for halide-free preparation of transition metal precursors and controlled addition of halides leads to ideal reproducibility and better understanding of some assembly processes. Furthermore, addition of catalytic amounts of halides provides mild sphere-formation procedures for the formation of novel materials.

■ ASSOCIATED CONTENT

Supporting Information

The Supporting Information is available free of charge at https://pubs.acs.org/doi/10.1021/acs.inorgchem.1c01714.

Experimental details on synthesis and characterization (^{1}H/^{13}C NMR and MS) (PDF)

https://doi.org/10.1021/acs.inorgchem.1c01714
Inorg. Chem. 2021, 60, 12498−12505

AUTHOR INFORMATION

Corresponding Author

Joost N. H. Reek − *van 't Hoff Institute for Molecular Sciences, University of Amsterdam, 1098 XH Amsterdam, The Netherlands;* orcid.org/0000-0001-5024-508X; Email: j.n.h.reek@uva.nl

Authors

Eduard. O. Bobylev − *van 't Hoff Institute for Molecular Sciences, University of Amsterdam, 1098 XH Amsterdam, The Netherlands*

Bas de Bruin − *van 't Hoff Institute for Molecular Sciences, University of Amsterdam, 1098 XH Amsterdam, The Netherlands;* orcid.org/0000-0002-3482-7669

Complete contact information is available at: https://pubs.acs.org/10.1021/acs.inorgchem.1c01714

Funding

We kindly acknowledge the University of Amsterdam for financial support to RPA sustainable chemistry.

Notes

The authors declare no competing financial interest.

ACKNOWLEDGMENTS

We would like to thank Bo Zhang for providing L^{4OMe}.

REFERENCES

(1) Yoshizawa, M.; Klosterman, J. K.; Fujita, M. Functional molecular flasks: new properties and reactions within discrete, self-assembled hosts. *Angew. Chem., Int. Ed.* **2009**, *48*, 3418−3438.

(2) Leenders, S. H. A. M.; Gramage-Doria, R.; de Bruin, B.; Reek, J. N. H. Transition metal catalysis in confined spaces. *Chem. Soc. Rev.* **2015**, *44*, 433−448.

(3) Han, M.; Engelhard, D. M.; Clever, G. H. Self-assembled coordination cages based on banana-shaped ligands. *Chem. Soc. Rev.* **2014**, *43*, 1848−1860.

(4) Fang, Y.; Powell, J. A.; Li, E.; Wang, Q.; Perry, Z.; Kirchon, A.; Yang, X.; Xiao, Z.; Zhu, C.; Zhang, L.; Huang, F.; Zhou, H.-C. Catalytic reactions within the cavity of coordination cages. *Chem. Soc. Rev.* **2019**, *48*, 4707−4730.

(5) Tan, C.; Chu, D.; Tang, X.; Liu, Y.; Xuan, W.; Cui, Y. Supramolecular Coordination Cages for Asymmetric Catalysis. *Chem.—Eur. J.* **2019**, *25*, 662−672.

(6) Zhang, D.; Ronson, T. K.; Zou, Y.-Q.; Nitschke, J. R. Metal−organic cages for molecular separations. *Nat. Rev. Chem.* **2021**, *5*, 168−182.

(7) Li, B.; He, T.; Fan, Y.; Yuan, X.; Qiu, H.; Yin, S. Recent developments in the construction of metallacycle/metallacage-cored supramolecular polymers via hierarchical self-assembly. *Chem. Commun.* **2019**, *55*, 8036−8059.

(8) Tranchemontagne, D. J.; Ni, Z.; O'Keeffe, M.; Yaghi, O. M. Reticular chemistry of metal-organic polyhedra. *Angew. Chem., Int. Ed.* **2008**, *47*, 5136−5147.

(9) Vardhan, H.; Yusubov, M.; Verpoort, F. Self-assembled metal−organic polyhedra: An overview of various applications. *Coord. Chem. Rev.* **2016**, *306*, 171−194.

(10) Fujita, D.; Ueda, Y.; Sato, S.; Yokoyama, H.; Mizuno, N.; Kumasaka, T.; Fujita, M. Self-Assembly of $M_{30}L_{60}$ Icosidodecahedron. *Chem* **2016**, *1*, 91−101.

(11) Sun, Q.-F.; Iwasa, J.; Ogawa, D.; Ishido, Y.; Sato, S.; Ozeki, T.; Sei, Y.; Yamaguchi, K.; Fujita, M. Self-assembled $M_{24}L_{48}$ polyhedra and their sharp structural switch upon subtle ligand variation. *Science* **2010**, *328*, 1144−1147.

(12) Suzuki, K.; Tominaga, M.; Kawano, M.; Fujita, M. Self-assembly of an M_6L_{12} coordination cube. *Chem. Commun.* **2009**, *13*, 1638−1640.

(13) Percástegui, E. G.; Ronson, T. K.; Nitschke, J. R. Design and Applications of Water-Soluble Coordination Cages. *Chem. Rev.* **2020**, *120*, 13480−13544.

(14) Yang, D.; Greenfield, J. L.; Ronson, T. K.; von Krbek, L. K. S.; Yu, L.; Nitschke, J. R. La(III) and Zn(II) Cooperatively Template a Metal-Organic Capsule. *J. Am. Chem. Soc.* **2020**, *142*, 19856−19861.

(15) Takezawa, H.; Shitozawa, K.; Fujita, M. Enhanced reactivity of twisted amides inside a molecular cage. *Nat. Chem.* **2020**, *12*, 574−578.

(16) Regeni, I.; Chen, B.; Frank, M.; Baksi, A.; Holstein, J. J.; Clever, G. H. Coal-Tar Dye-based Coordination Cages and Helicates. *Angew. Chem., Int. Ed.* **2021**, *60*, 5673−5678.

(17) Chen, L.; Yang, T.; Cui, H.; Cai, T.; Zhang, L.; Su, C.-Y. A porous metal−organic cage constructed from dirhodium paddle-wheels: synthesis, structure and catalysis. *J. Mater. Chem. A* **2015**, *3*, 20201−20209.

(18) Jaya Prakash, M.; Oh, M.; Liu, X.; Han, K. N.; Seong, G. H.; Lah, M. S. Edge-directed $[(M_2)_2L_4]$ tetragonal metal-organic polyhedra decorated using a square paddle-wheel secondary building unit. *Chem. Commun.* **2010**, *46*, 2049−2051.

(19) Fiedler, D.; Bergman, R. G.; Raymond, K. N. Stabilization of reactive organometallic intermediates inside a self-assembled nanoscale host. *Angew. Chem., Int. Ed.* **2006**, *45*, 745−748.

(20) Fiedler, D.; Leung, D. H.; Bergman, R. G.; Raymond, K. N. Selective molecular recognition, C-H bond activation, and catalysis in nanoscale reaction vessels. *Acc. Chem. Res.* **2005**, *38*, 349−358.

(21) Leung, D. H.; Fiedler, D.; Bergman, R. G.; Raymond, K. N. Selective C-H bond activation by a supramolecular host-guest assembly. *Angew. Chem., Int. Ed.* **2004**, *43*, 963−966.

(22) Gan, M.-M.; Liu, J.-Q.; Zhang, L.; Wang, Y.-Y.; Hahn, F. E.; Han, Y.-F. Preparation and Post-Assembly Modification of Metallosupramolecular Assemblies from Poly(N-Heterocyclic Carbene) Ligands. *Chem. Rev.* **2018**, *118*, 9587−9641.

(23) Ibáñez, S.; Poyatos, M.; Peris, E. N-Heterocyclic Carbenes: A Door Open to Supramolecular Organometallic Chemistry. *Acc. Chem. Res.* **2020**, *53*, 1401−1413.

(24) Sinha, N.; Hahn, F. E. Metallosupramolecular Architectures Obtained from Poly-N-heterocyclic Carbene Ligands. *Acc. Chem. Res.* **2017**, *50*, 2167−2184.

(25) Bobylev, E. O.; Poole, D. A., III; de Bruin, B.; Reek, J. N. H. Selective formation of $Pt_{12}L_{24}$ nanospheres by ligand design. *Chem. Sci.* **2021**, *12*, 7696−7705.

(26) Li, Z.; Kishi, N.; Hasegawa, K.; Akita, M.; Yoshizawa, M. Highly fluorescent M_2L_4 molecular capsules with anthracene shells. *Chem. Commun.* **2011**, *47*, 8605−8607.

(27) Li, Z.; Kishi, N.; Yoza, K.; Akita, M.; Yoshizawa, M. Isostructural M_2L_4 molecular capsules with anthracene shells: synthesis, crystal structures, and fluorescent properties. *Chem.—Eur. J.* **2012**, *18*, 8358−8365.

(28) Martí-Centelles, V.; Lawrence, A. L.; Lusby, P. J. High Activity and Efficient Turnover by a Simple, Self-Assembled "Artificial Diels-Alderase". *J. Am. Chem. Soc.* **2018**, *140*, 2862−2868.

(29) Spicer, R. L.; Stergiou, A. D.; Young, T. A.; Duarte, F.; Symes, M. D.; Lusby, P. J. Host-Guest-Induced Electron Transfer Triggers Radical-Cation Catalysis. *J. Am. Chem. Soc.* **2020**, *142*, 2134−2139.

(30) Gonell, S.; Caumes, X.; Orth, N.; Ivanović-Burmazović, I.; Reek, J. N. H. Self-assembled $M_{12}L_{24}$ nanospheres as a reaction vessel to facilitate a dinuclear Cu(i) catalyzed cyclization reaction. *Chem. Sci.* **2019**, *10*, 1316−1321.

(31) Yan, X.; Wei, P.; Liu, Y.; Wang, M.; Chen, C.; Zhao, J.; Li, G.; Saha, M. L.; Zhou, Z.; An, Z.; Li, X.; Stang, P. J. Endo- and Exo-Functionalized Tetraphenylethylene $M_{12}L_{24}$ Nanospheres: Fluorescence Emission inside a Confined Space. *J. Am. Chem. Soc.* **2019**, *141*, 9673−9679.

(32) Leenders, S. H. A. M.; Dürr, M.; Ivanović-Burmazović, I.; Reek, J. N. H. Gold Functionalized Platinum $M_{12}L_{24}$-Nanospheres and Their Application in Cyclization Reactions. *Adv. Synth. Catal.* **2016**, *358*, 1509−1518.

(33) Kaiser, F.; Schmidt, A.; Heydenreuter, W.; Altmann, P. J.; Casini, A.; Sieber, S. A.; Kühn, F. E. Self-Assembled Palladium and Platinum Coordination Cages: Photophysical Studies and Anticancer Activity. *Eur. J. Inorg. Chem.* **2016**, *2016*, 5189−5196.
(34) Pöthig, A.; Casini, A. Recent Developments of Supramolecular Metal-based Structures for Applications in Cancer Therapy and Imaging. *Theranostics* **2019**, *9*, 3150−3169.
(35) Bobylev, E. O.; Poole, D. A., III; Bruin, B.; Reek, J. N. H. How to prepare kinetically stable self-assembled $Pt_{12}L_{24}$ nanospheres circumventing kinetic traps. *Chem.—Eur. J.* **2021**, 27 DOI: 10.1002/chem.202101931.
(36) Kai, S.; Shigeta, T.; Kojima, T.; Hiraoka, S. Quantitative Analysis of the Self-Assembly Process of a $Pd_{12}L_{24}$ Coordination Sphere. *Chem.—Asian. J.* **2017**, *12*, 3203−3207.
(37) Zhukhovitskiy, A. V.; Zhong, M.; Keeler, E. G.; Michaelis, V. K.; Sun, J. E. P.; Hore, M. J. A.; Pochan, D. J.; Griffin, R. G.; Willard, A. P.; Johnson, J. A. Highly branched and loop-rich gels via formation of metal-organic cages linked by polymers. *Nat. Chem.* **2016**, *8*, 33−41.
(38) Jiang, Y.; Zhang, H.; Cui, Z.; Tan, T. Modeling Coordination-Directed Self-Assembly of M_2L_4 Nanocapsule Featuring Competitive Guest Encapsulation. *J. Phys. Chem. Lett.* **2017**, *8*, 2082−2086.
(39) Kishi, N.; Li, Z.; Yoza, K.; Akita, M.; Yoshizawa, M. An M_2L_4 Molecular Capsule with an Anthracene Shell: Encapsulation of Large Guests up to 1 nm. *J. Am. Chem. Soc.* **2011**, *133*, 11438−11441.
(40) Fujita, D.; Takahashi, A.; Sato, S.; Fujita, M. Self-assembly of Pt(II) spherical complexes via temporary labilization of the metal-ligand association in 2,2,2-trifluoroethanol. *J. Am. Chem. Soc.* **2011**, *133*, 13317−13319.
(41) Puig, E.; Desmarets, C.; Gontard, G.; Rager, M. N.; Cooksy, A. L.; Amouri, H. Capturing a Square Planar Gold(III) Complex Inside a Platinum Nanocage: A Combined Experimental and Theoretical Study. *Inorg. Chem.* **2019**, *58*, 3189−3195.
(42) Zaffaroni, R.; Bobylev, E. O.; Plessius, R.; van der Vlugt, J. I.; Reek, J. N. H. How to Control the Rate of Heterogeneous Electron Transfer across the Rim of M_6L_{12} and $M_{12}L_{24}$ Nanospheres. *J. Am. Chem. Soc.* **2020**, *142*, 8837−8847.
(43) Percástegui, E. G.; Mosquera, J.; Ronson, T. K.; Plajer, A. J.; Kieffer, M.; Nitschke, J. R. Waterproof architectures through subcomponent self-assembly. *Chem. Sci.* **2019**, *10*, 2006−2018.
(44) Komine, S.; Tateishi, T.; Kojima, T.; Nakagawa, H.; Hayashi, Y.; Takahashi, S.; Hiraoka, S. Self-assembly processes of octahedron-shaped P_d6L_{12} cages. *Dalton Trans.* **2019**, *48*, 4139−4148.
(45) Takahashi, S.; Sasaki, Y.; Hiraoka, S.; Sato, H. A stochastic model study on the self-assembly process of a Pd_2L_4 cage consisting of rigid ditopic ligands. *Phys. Chem. Chem. Phys.* **2019**, *21*, 6341−6347.

https://doi.org/10.1021/acs.inorgchem.1c01714
Inorg. Chem. 2021, 60, 12498−12505